

LEI SHI <sup>\*</sup>, WEIYONG LU <sup>1,2</sup>, DONG LV <sup>3,4</sup>**ROCK BREAKING MECHANISM AND PROCESS OPTIMISATION OF JET CUTTING BASIC ROOF ROCK UNDER SUBMERGED JET CONDITION**

The destruction of rock under the condition of a close submerged jet has become a hot topic of scientific research and engineering application in the past decade. With the unremitting efforts of a large number of experts and scholars around the world, gratifying progress has been made in the research of computational fluid dynamics (CFD) on the internal and external flow fields of the jet nozzle, the theoretical derivation of rock mechanics on the fracture initiation and propagation criteria of hydraulic fracturing, and the numerical simulation of jet erosion mechanism under the coupling of fluid and solid fields, however, for the rock mechanics hydraulic fracturing cutting engineering scale of non-oil drilling fracturing technology, the research on the fluid-solid coupling boundary conditions of fracturing fluid and hard dense rock under the flow state conditions of the submerged field inside and outside the borehole is not sufficient. In the calculation of the fluid-solid coupling boundary flow field under the non-submerged jet state, the control equation with Reynolds number between 2300-4000 shall be selected, while it belongs to the laminar flow state in the stage of hole sealing and pressurised fracturing. Therefore, Von-Mises equivalent plastic stress is selected in the mechanical model to calibrate the failure state of the rock-solid boundary, and the control equations of laminar flow and turbulent flow are selected to calibrate the fluid boundary. The mechanism of different stages of rock breaking by hydraulic fracturing jet can be further analysed in detail, and Comsol 6.0 multi-physical field simulation software is selected for verification. The research results will help deepen the understanding of rock breaking mechanism by jet and optimise the selection of parameters for field construction.

**Keywords:** Turbulence effect; Multi physical field simulation; Fluid solid coupling; High pressure water jet

<sup>1</sup> LYULIANG UNIVERSITY, DEPARTMENT OF MINING ENGINEERING, LVLIANG, SHANXI 033001, CHINA

<sup>2</sup> LVLIANG ENGINEERING RESEARCH CENTER OF INTELLIGENT COAL MINE, LVLIANG, SHANXI 033001, CHINA

<sup>3</sup> INNER MONGOLIA ENERGY GROUP CO., LTD., HOHHOT, INNER MONGOLIA 010090, CHINA

<sup>4</sup> INNER MONGOLIA TONGSHENG SELIAN COAL DEVELOPMENT CO., LTD. ORDOS, INNER MONGOLIA 014399, CHINA

\* Corresponding author: [cumtshilei@163.com](mailto:cumtshilei@163.com)



© 2024. The Author(s). This is an open-access article distributed under the terms of the Creative Commons Attribution-NonCommercial License (CC BY-NC 4.0, <https://creativecommons.org/licenses/by-nc/4.0/deed.en>) which permits the use, redistribution of the material in any medium or format, transforming and building upon the material, provided that the article is properly cited, the use is noncommercial, and no modifications or adaptations are made.

## 1. Introduction

Hydraulic fracturing refers to a technology in which material cracks rupture and expand due to the pressure of its internal liquid. In 1947, it was first applied in the Hugoton oil and gas field vertical well fracturing stimulation project in the southwest of Kansas, the United States [1]. After more than 70 years of development and exploration, hydraulic fracturing technology has become a major and reliable measure for the purpose of rock material destruction, such as natural gas extraction, oil and gas well stimulation and injection [2]. The direction and length of crack initiation, propagation and development, as well as the interaction effect between three-dimensional cracks in materials have been studied and put into practice. The origin of high-pressure water jet technology is in the mining industry. In the 1930s, a water jet was used to flush coal seams in coal mines. In the early 1950s, the former Soviet Union used high-pressure pure water jets to drill granite bedrock [3]; Johnson V.E. Jr. [4] of the United States studied the optimisation of the relationship between jet nozzle structure, target distance, moving speed, and eroded rock material by the end of the 1980s [5]. The cutting efficiency of high-pressure water jet drilling was then increased by nearly 49.3%.

Hydraulic fracturing and high-pressure water jet cutting have a wide range of application fields, such as the cutting of ship decks, the repair and reconstruction of the basic bearing structure of ancient buildings with protection value, computer heat dissipation, and the rock cutting and destruction of coal mines that are difficult to use explosive blasting [6-7]. Therefore, it has always been the focus of attention of experts, scholars and engineers at home and abroad. Because it involves the interaction relationship between two materials with different properties of fluid and solid, the properties and states of the two materials have apparent changes in different stages, which makes it difficult for theoretical mechanical calculation and numerical simulation experiments to accurately describe the action process [8]. In the past nearly 60 years of research history, numerous overseas experts have provided us with a good work foundation and vision [9].

Researchers have applied a variety of research methods to various directions of hydraulic fracturing and high-pressure water jet cutting:

Bu Y.H. et al. [10] compared the rock-breaking experiments of the rotary jet and ordinary round jet and found that the rotary jet is superior to the ordinary round jet in the minimum threshold of rock-breaking pressure, breaking area and drilling forming degree. Raju S.P. [11] used an integral equation to describe the time average velocity of the internal and external flow field of the ejector at the space-time scale and compared and optimised the nozzle shape. Chigier and Chervinsky [12] conducted theoretical research on the external flow field of the jet under the turbulent state and established the integral control equation of the turbulent flow field of the rotating jet by using the assumption of approximate laminar flow of the boundary layer. By 2015, Wang Y.F. [13] further deduced the control equations of the internal and external flow fields of the nozzle under submerged jet conditions and compared the rock-breaking effects of submerged jet and non-submerged jet under laboratory conditions.

Scholars at home and abroad have conducted a lot of in-depth research on the experimental engineering of fluid-solid coupling multi-physical fields in the past three decades, and MIT's Bate [14] successfully developed the experimental calculation method of fluid-solid coupling problem in commercial software; Choi [15], etc. used the method of separating variables to solve the mixed equation of the fluid-solid coupling problem, adopted the four-step method and ale technology, and cited the symmetric pressure equation.

In this paper, based on the exceptional achievements made by domestic and foreign experts and scholars, the submerged jet flow field and the solid mechanical boundary state under the engineering scale will be further reproduced through the fluid solid coupling multi-physical field finite element analysis, and the rock jet erosion damage parameters applicable to specific conditions will be obtained by comparing the effects of different shape jet nozzles on the turbulent fluid in the flow field and on the solid boundary, It provides a simple method for the application of rock mechanics in coal mine.

## 2. Establishment of multi physical field simulation model and structure of ejector

The internal space between the ejector and the borehole wall under the submerged jet state belongs to the slit [16-19]. Even if the internal pressure of the slit is very small when connecting the free and open outlet, the conditions for the occurrence of turbulent state may be met. The specific discrimination conditions are given by Poiseuille's law, laminar flow flux formula and turbulent steady-state control equation [20]:

$$Q = \Delta P / \left[ 8\eta L \cdot (\pi r^4) \right] \quad (1)$$

$$q = -\frac{w^3}{\mu'} \nabla P_f \quad (2)$$

$$P_f \cdot S \frac{\partial P_f}{\partial t} + \nabla \cdot (P_f \cdot V) = -P_f \alpha_B \frac{\partial}{\partial t} \varepsilon_{vol} \quad (3)$$

Where,  $Q$  represents flow rate,  $m^3/s$ ;  $\Delta P$  represents the increment of fluid pressure, MPa;  $\eta$  is the capacity factor;  $L$  is the distance travelled by the fluid, m;  $r$  is the aperture, m;  $q$  is Boyle's law constant;  $\omega$  is the motor speed of high-pressure water pump, times/s;  $S$  is the distance length of the fluid doing work, m.

The above equations (1), (2) and (3) are substituted into the Reynolds number calculation formula for calculation, wherein the geometric dimension  $r$  of the drilling slit is about  $5 \times 10^{-3}$  m. Dynamic viscosity coefficient of fracturing fluid  $\mu$  about  $1.088 \times 10^{-6}$  kPa/s, the calculation shows that when the head pressure exceeds 5 MPa in the submerged state, the internal flow field of the borehole is divided into turbulence, and when the water injection pressure further rises, the packer works by maintaining a constant pressure and then returns to the laminar flow state. Therefore, the transient solver should be selected for the distribution solution when studying the jet rock breaking-process. The turbulence  $k$ - $\varepsilon$  [21] 's transient control equation is as follows:

$$\begin{cases} \rho \frac{\partial u}{\partial t} + \rho (u_2 \cdot \nabla) u_2 = \nabla \cdot [-p_{2l} + \kappa] + F \\ \rho \nabla \cdot u_2 = 0 \end{cases} \quad (4)$$

$$\kappa = (\mu + \mu_T) \left( \nabla u_2 + (\nabla u_2)^T \right) \quad (5)$$

$$\rho \frac{\partial k_2}{\partial t} + \rho(u_2 \cdot \nabla)k_2 = \nabla \cdot \left[ \left( \mu + \frac{\mu_T}{\sigma_K} \right) \nabla k_2 \right] + P_k - \rho \varepsilon \quad (6)$$

$$\begin{aligned} \rho \frac{\partial \varepsilon}{\partial t} + \rho(u_2 \cdot \nabla)\varepsilon = \nabla \cdot \left[ \left( \mu + \frac{\mu_T}{\sigma_\varepsilon} \right) \nabla \varepsilon \right] + \\ + C_{\varepsilon 1} \frac{\varepsilon}{k_2} P_k - C_{\varepsilon 2} \rho \frac{\varepsilon^2}{k_2}, \quad \varepsilon = \varepsilon p_2 \end{aligned} \quad (7)$$

$$\mu_T = \rho C_\mu \frac{k_2^2}{\varepsilon}, \quad P_k = \mu_T \left[ \nabla u_2 : \left( \nabla u_2 + (\nabla u_2)^T \right) \right] \quad (8)$$

Where  $u_2$  is the velocity field component, m/s;  $P$  is the pressure, MPa;  $k_2$  is the turbulent flow energy, n·m;  $\varepsilon$  is the turbulent dissipation rate;  $\rho$  is the fluid density, kg·m<sup>-3</sup>;  $\nabla$  is the symbol of Nabutchin operator;  $\kappa$  is a direction gradient matrix,  $\mu$  is the dynamic viscosity coefficient, n·s/m<sup>3</sup>;  $T$  is the space tensor matrix

Three experimental models are designed to compare the difference in turbulent flow field distribution caused by different nozzle shapes according to the common structural forms of the jet in hydraulic fracturing of sandstone, granite and other hard rock layers at the construction site, as shown in Fig. 1. According to jet symmetry [22], three jet nozzle structure models are established: I. conical straight nozzle model; II. V-shaped Swirling Nozzle model; III. Conical necked nozzle model, as shown in Fig. 1(a)-(c). In order to control the experimental variables, the length of the steady laminar flow stage is 5 m, the length of the pressurisation acceleration contraction stage is 0.05 m, the length of the internal nozzle of the jet is 0.1 m, the outer diameter of the jet is 0.75 m, and the drilling diameter is 0.8 m; The inlet pressure of the flow field is 50 MPa, the inner wall is a non-slip rigid body, and the outlet is an open outlet that is fully developed and inhibits backflow.

According to the grid division function of comsol 6.0, by comparing the convergence of 0.1-0.4 mm scale grids [23], it is determined that the quality of the 0.2 mm grid is high, and the fluid-solid coupling boundary is set as the hydrodynamic calculation law based on the laminar flow control equation, which is conducive to the stability of the experimental results [24]. The grid partitioning method adopts the partitioning principle of iteratively selecting the optimal adaptive mechanical equation in version 6.0, and the time step calculation mode is 1e-3s.

In practical engineering applications, the interaction between the high-pressure and high-speed fluid ejected by the high-pressure jet and the solid mechanical rock material can be divided into four stages [25-28]:

Stage I Water injection stage of jet: After the directional drill pipe is taken out, the jet packer is drilled into the target position by the fracturing drill pipe, and the high-pressure water pump transfers the fracturing fluid to the jet at a certain flow rate and pressure until the drill pipe vibrates, and the fracturing fluid returns from the bottom of the drill hole and is discharged from the orifice;

Stage II pressure holding stage of the jet: After the completion of the erosion and rock breaking operation, the packer is inflated with water, and the fracturing operation is started. The internal flow rate of the packer is basically zero, and the pressure is kept constant within a certain range.

Stage III erosion and rock breaking stage: Before the packer works, the high-pressure water pump continues to pressurise, and the flow increases, causing the fracturing fluid to rapidly

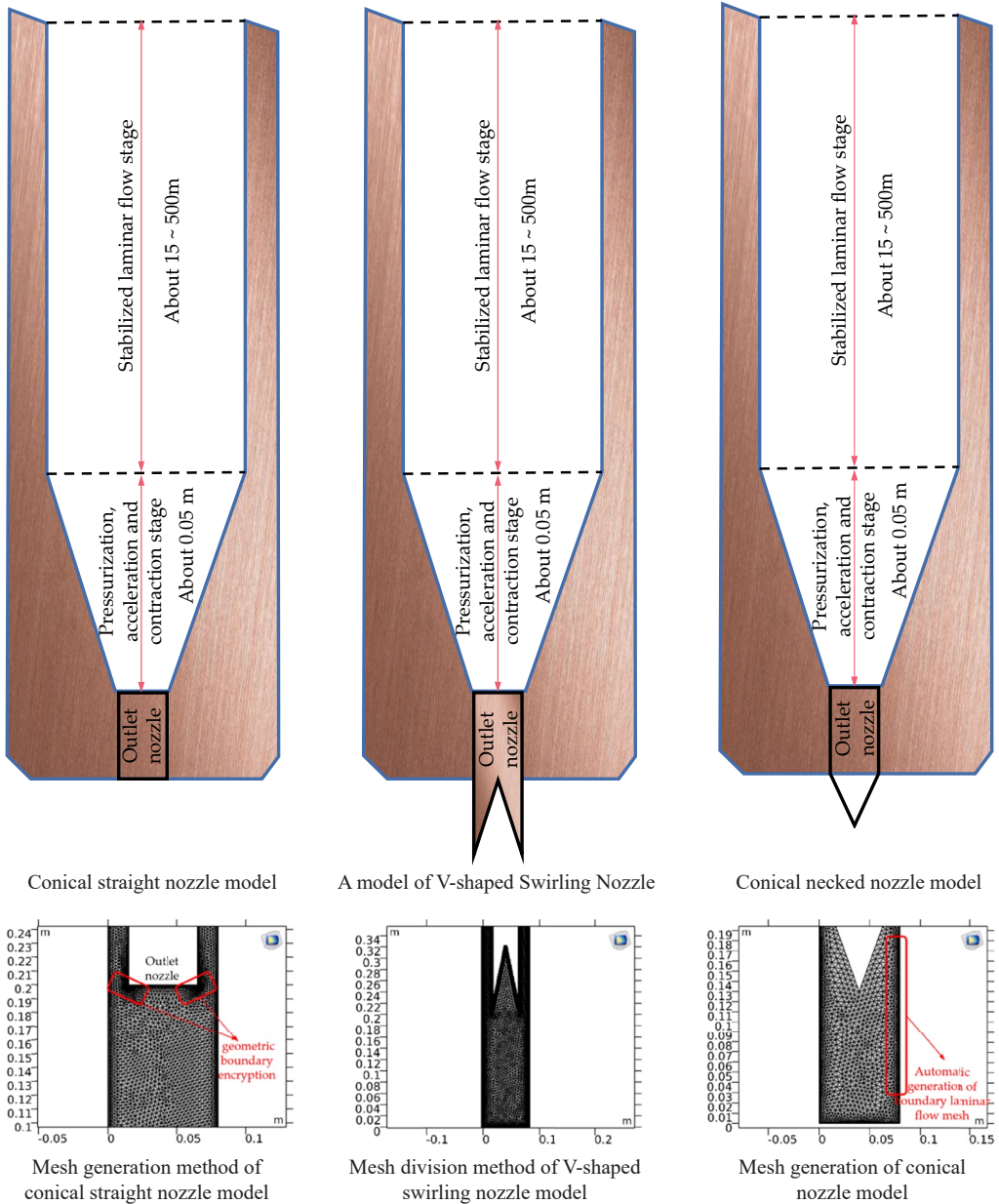


Fig. 1. Structure and mesh division of high pressure jet nozzle

impact the rock surface, destroying the integrity of the rock by erosion, grinding and shearing to achieve the purpose of cutting and inducing fractures.

Stage IV under certain conditions, the variable-frequency motor high-pressure water pump will be used to conduct jet cutting and fracturing on the rock that is difficult to damage in the

form of a pulse jet. In this case, the internal flow field of the drill pipe will always change repeatedly in the state of pressure holding and free opening, so the flow field status remains critical flow or turbulence.

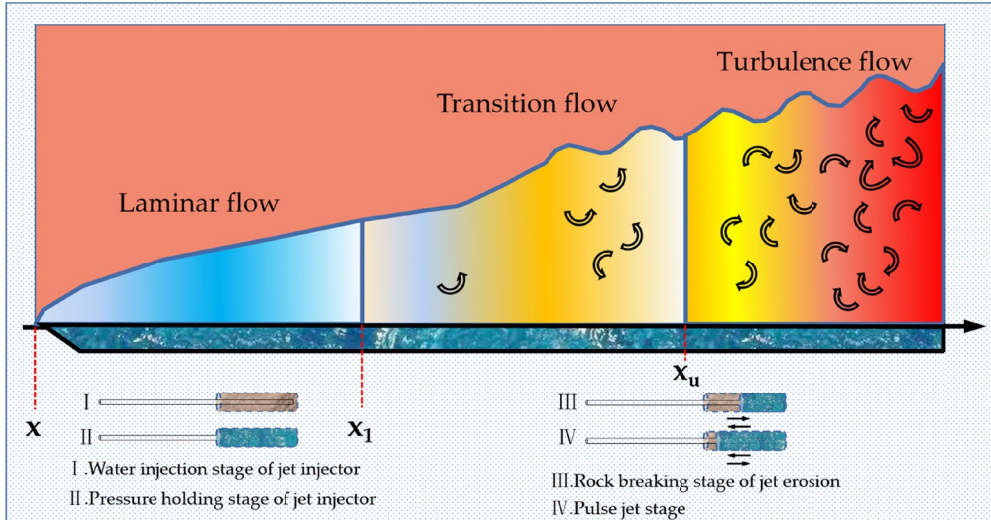


Fig. 2. Internal flow field state of jet ejector in different stages

Then, the dense and hard medium-grained sandstone, which is typical and common in the basic roof rock, is selected to represent the target body of jet rock breaking and erosion. When hard conglomerate roof is rarely encountered, the research conclusion of tight sandstone can be further analogized to other types of roof conditions. The elastic modulus  $E$  is 7.07 GPa, and the density  $\rho$  2560 kg/m<sup>3</sup>, cohesion is 2.5 MPa. The geometric dimension is 5×5 m, drill holes at the centre of the top of the test piece at the coordinates of (2.5, 2.5, 5), the hole depth is 1 m, the hole diameter is 0.08 m, and the internal depth is 0.075 m.

The uniformly distributed load of 10 MPa loaded on the top is:  $\sigma_V$  vertical stress; 15 MPa horizontal maximum principal stress applied on both sides of  $Y$  direction  $\sigma_H$ . Apply 12 MPa horizontal minimum principal stress in  $X$  direction  $\sigma_h$ . As shown in Fig. 3.

### 3. Results and analysis of fluid solid coupling simulation experiment

Based on the above experimental scheme and the divided mechanical model grid structure [29-31], the hypothetical conditions and calculation probes in the multi-physical field fluid-solid coupling experiment are set, so that the convergence of the experimental results can reach within 1E-05. When the reference temperature  $K$  is set to 25°C, and the reference pressure level  $spf.pref$  as 1atm, the time step CFL as 0.1 s, the turbulence length  $l_T$  is automatically selected based on the geometric length, the turbulence intensity  $L_T$  is selected as 0.05 medium turbulence intensity,

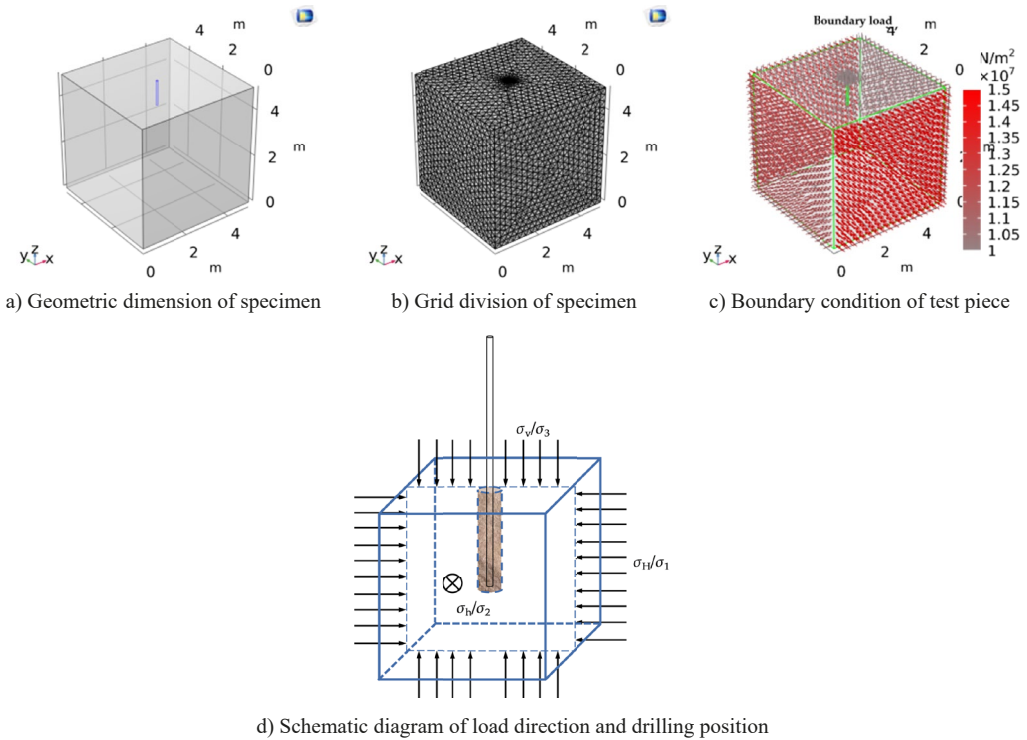


Fig. 3. Geometric mesh generation of three-dimensional specimen & boundary load conditions

and the normal backflow is suppressed. Based on the above conditions, the turbulence dissipation rate can be obtained  $\varepsilon$  and turbulent kinetic energy  $k_2$ :

$$\varepsilon = C_\mu^{3/4} \frac{k_2^{3/2}}{L_T}, \quad k_2 = \frac{3}{2} (U_{ref} l_T)^2 \quad (9)$$

The fluid velocity and equivalent Von-Mises stress on the fluid-solid coupling boundary surface are shown in Fig. 4.

It can be seen from the comparison of the surface velocity field of the fluid-solid coupling boundary in Fig. 4a-b-c show that the flow field inside the boreholes of the nozzle jet of the three structures has a turbulence calculation singularity [32], which exceeds  $1E8$  m/s, and it is difficult to appear on the engineering scale. This is because the turbulence effect causes the air movement speed of the inclusion in the fluid to exceed Mach 4, resulting in the calculation step length CFL 0.1 is no longer suitable for convergence. However, selecting a smaller time step is more disadvantageous to the accuracy of the calculation results. Therefore, when analysing the experimental results, the influence of singularity is excluded, and only the middle range of the threshold is compared, which is also the case when comparing the equivalent stress.

It can be seen that the average velocity of the flow field of the type II nozzle is the highest. According to the results stored by the probe, it should be  $0.76E8$  m/s. The peak velocity of the flow field of the type III nozzle is the highest, but the average value is slightly lower than that of

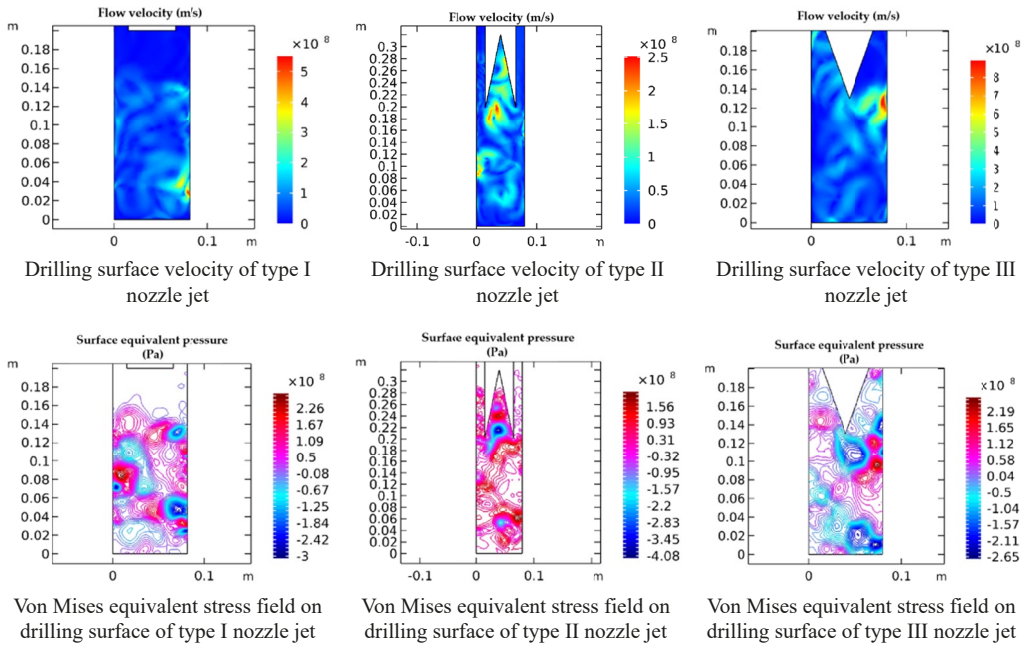


Fig. 4. Mechanical state of fluid-solid coupling boundary in two field coupling experiment

the type II nozzle, both of which are better than the type I nozzle. The higher the flow velocity of the flow field on the surface of the fluid-solid coupling boundary, the more apparent the erosion effect of the internal fluid on the rock surface. Therefore, from the perspective of the effect of erosion and rock breaking, a Type II / III nozzle is more suitable. The roof-cutting test for the type II nozzle was carried out on the S1201-II working face of a mine in Shaanxi. The results show that under the conditions of jet pressure 25 MPa, nozzle diameter 1.5 mm, abrasive type yellow sand/quartz sand, abrasive mass concentration 3.5% and cutting speed 4.4 mm/s, the developed system can make slits at the same time in 4 holes of 7000-8000 mm deep within a cycle time (50 min).

Comparing the surface equivalent stress field of d-e-f Von-Mises boreholes in Fig. 4 is straightforward. It can be seen that the average value of the surface equivalent stress field of type II boreholes is  $1.25E8$  MPa, which is much larger than the  $0.33E8$  MPa and  $0.52E8$  MPa of type I and type III boreholes. The magnitude of the surface stress field is mainly reflected in the jet mechanism of rock destruction by tension water wedge and dense core splitting. There is a stress difference between the high-stress concentration area and the adjacent area. From the point of view of equivalent stress, it can be concluded that the jet device with a type II nozzle has a better effect on the initiation and propagation of rock cracks than type I / III cracks.

## 4. Conclusion

Based on the established multi-physical field fluid-solid coupling mechanical model, combined with the relevant definitions and assumptions in computational fluid mechanics and rock

mechanics, the mechanical models of the interaction between the internal flow field and rock of the three types of structure jets are established. The experimental conditions, the governing equations of turbulent computational fluid mechanics and the constitutive equations of rock mechanics are set up. According to the results of numerical simulation and theoretical calculation, based on the equivalent stress magnitude on the rock surface, the influence weight of nozzle shape structure is greater than the influence of drilling flow volume.

The comparison results of the flow velocity and the surface equivalent stress under certain conditions under the simulated engineering scale are obtained. According to the analysis of the experimental results, some further inferences about the field construction and the structural design of the jet can be obtained:

- (1) In the structural design of the jet generator, the swirler with little influence on the flow velocity shall be added as much as possible, and the nozzle structure shall have as many inlets with parallel jet directions as possible to improve the erosion effect of the turbulence effect in the flow field on the rock surface;
- (2) In the rock-breaking stage of the jet machine, the sand carrying fracturing fluid can be selected to further increase the erosion effect of the high-pressure jet on the rock surface and can be used as a proppant for fracture expansion in the fracturing stage;
- (3) During on-site construction, the effect of increasing the pump pressure to a higher level in the high-pressure jet stage is not obvious. Instead, the flow rate and drill pipe diameter should be increased to cooperate with the type II nozzle jet to cut the hard and smooth surface rock.

### Data Availability

The experimental and analytical calculation results data used to support the findings of this study are included within the article.

### Conflicts of Interest

The authors declare that there are no conflicts of interest regarding the publication of this paper.

### Acknowledgments

This work was supported by the Fundamental Research Program of Shanxi Province (No. 20210302124633), Supported by the Introduction Plan of High-Level Scientific and Technological Talents in Lvliang City (ShiLei), Science and technology innovation plan innovation platform project of Shanxi University (2022P024), Science and Technology Project of Lvliang City in 2022 (2022GXZF08), Supported by Scientific and Technological Innovation Programs of Higher Education Institutions in Shanxi (2022L560), Education and Teaching Reforms Project of Graduate Students in Shanxi Province (2022YJJG305), the Lvliang Platform base construction project (No. 2021GCZX-1-46).

At the same time, we also need to thank the following funds for their strong support in the research, experiment and writing of this paper: the Natural Science Foundation of Fujian Province (Grant No. 2022J05261), the Fujian science and technology plan project (Guiding project) (Grant No. 2020Y0092), the Wuyi University introduced talents and started scientific research project (Grant No. YJ202202).

## References

- [1] M.K. Hubbert, D. Willis, Mechanics of hydraulic fracturing. *Transactions of the AIME* **18** (1), (1972). DOI: <https://doi.org/10.1146/annurev-fluid-010814-014736>
- [2] A. Ellsworth, L. William, Injection-Induced Earthquakes. *Science*, (2013). DOI: <https://doi.org/10.1126/science.1225942>
- [3] Jiang Ruizhong, Jiang Tingxue, & Wang Yongli, The recent development and prospects of hydraulic fracturing technology *Petroleum Drilling and Production Technology* **26** (004), 52-57 (2004).
- [4] V.E. Johnson, G.L. Chahine, A.F. Conn et al., Cavitating and Structured Jets for Mechanical Bits to Increase Drilling Rate – Part I: Theory and Concepts. *Journal of Energy Resources Technology* **106** (2), (1984). DOI: <https://doi.org/10.1115/1.3231053>
- [5] J.I. Adachi, E. Siebrits, A.P. Peirce et al., Computer simulation of hydraulic fractures. *International Journal of Rock Mechanics and Mining Sciences* **44** (5), 739-757 (2007). DOI: <https://doi.org/10.1016/j.ijrmms.2006.11.006>
- [6] W.D. Norman, R.J. Jasinski, E.B. Nelson, Hydraulic fracturing process and compositions. US (1996).
- [7] R.Z. Jiang, T.X. Jiang, Y.L. Wang, Recent development and Prospect of hydraulic fracturing technology. *Petroleum Drilling and Production Technology* (04), 52-57 + 84 (2004). DOI: <https://doi.org/10.13639/j.odpt.2004.04.019>
- [8] J. Wang, G. Li, H. Zhao et al., Stability Analysis of a Borehole Wall during Horizontal Directional Drilling in Fluid-Solid Coupling Condition. *Chinese Journal of Underground Space and Engineering* (2012). DOI: <https://doi.org/10.1016/j.tust.2007.01.002>
- [9] J. Liu, Study of fluid-solid coupling flow in low permeable oil reservoir. *Chinese Journal of Rock Mechanics and Engineering* **21** (1), 88-92. DOI: [https://doi.org/10.1016/S0731-7085\(02\)00079-1](https://doi.org/10.1016/S0731-7085(02)00079-1)
- [10] Y.H. Bu, R.H. Wang, W.D. Zhou, Study on the flow law of rotating jet. *Petroleum Drilling and Production Technology* (02), 7-10 + 105 (1997). DOI: <https://doi.org/10.13639/j.odpt.1997.02.002>. DOI: <https://doi.org/10.1007/BF03182422>
- [11] S.P. Raju, M. Ramulu, Predicting hydro-abrasive erosive wear during abrasive waterjet cutting (1994). DOI: <https://doi.org/10.3390/en15062028>
- [12] N.A. Chigier, A. Chervinsky, Experimental Investigation of Swirling Vortex Motion in Jets. *Journal of Applied Mechanics* **34** (2) (1967). DOI: <https://doi.org/10.1115/1.3607703>
- [13] Y.F. Wang, Research on three-dimensional rotating water jet combined with hydraulic fracturing technology. *China University of Mining and Technology* (2015). DOI: <https://doi.org/10.1515/jag-2019-0032>
- [14] K.J. Bathe, Z. Hou, S. Ji, Finite element analysis of fluid flows fully coupled with structural interactions. *Computers & Structures* **72** (1-3), 1-16 (1999). DOI: [https://doi.org/10.1016/S0045-7949\(99\)00042-5](https://doi.org/10.1016/S0045-7949(99)00042-5)
- [15] H.G. Choi, D.D. Joseph, Abstract Fluidization by lift of 300 circular particles in plane Poiseuille flow by direct numerical simulation. *Journal of Fluid Mechanics* **438**, 101-128 (2001). DOI: <https://doi.org/10.1017/S0022112001004177>
- [16] B.E. Launder et al., The numerical computation of turbulent flows – ScienceDirect. *Computer Methods in Applied Mechanics and Engineering* **3** (2), 269-289 (1974). DOI: <https://doi.org/10.1016/j.jweia.2008.01.011>
- [17] Y. Lu, J. Tang, Z. Ge, B. Xia, Y. Liu, Hard rock drilling technique with abrasive water jet assistance. *International Journal of Rock Mechanics & Mining Sciences* **60**, 47-56 (2013).
- [18] A.M. Dimits, G. Bateman, M.A. Beer, B.I. Cohen, W. Dorland, G.W. Hammett et al., Comparisons and physics basis of tokamak transport models and turbulence simulations. *Physics of Plasmas* **7** (3), 969-983 (2000).
- [19] Y. He, W. Ma, C. Liu, Numerical Simulation on CFD of Flow Field in Hydrodynamic Coupling and Characteristics Prediction. *Asia-pacific Power & Energy Engineering Conference. IEEE* (2009).
- [20] T.J. Poinso et al., Boundary conditions for direct simulations of compressible viscous flows. *Journal of Computational Physics* (1992). DOI: <https://doi.org/10.1016/j.jcp.2008.01.038>
- [21] I. Y. Zhang, S.Y. Liu, B.G. Wang, Application of Reynolds stress model in three-dimensional turbulent flow field calculation. *Journal of Aeronautical dynamics* (04), 572-576 (2005). DOI: <https://doi.org/10.13224/j.cnki.jasp.2005.04.009>
- [21] Y.D. Li, Y. B. Cai, Y.L. Zhang, W.F. Sun, Optimization of nozzle structure of three-dimensional rotary jet gun. *Hydraulic and Pneumatic* (10), 40-43 (2015). DOI: <https://doi.org/10.20964/2020.09.37>

- [22] M. Hassanizadeh, W.G. Gray, General conservation equations for multi-phase systems: 1. Averaging procedure. *Advances in Water Resources* **3** (1), 25-40 (1979). DOI: <https://doi.org/10.1016/j.jcp.2008.01.038>
- [23] W. Zhang, J. Sun, Z.Q. Qu, T.K. Guo, F.C. Gong, H.Y. Zhang, Thermal fluid solid coupling model and comprehensive evaluation method for high temperature geothermal exploitation. *Progress in Geophysics* **34** (02), 668-675 (2019). DOI: <https://doi.org/10.3901/CJME.2014.0529.107>
- [24] G.S. Li, Z.H. Shen, Research progress of high pressure water jet theory and its application in petroleum engineering. *Petroleum Exploration and Development* (01), 96-99 (2005). DOI: <https://doi.org/10.1155/2021/6647500>
- [25] A.W. Momber, R. Kovacevic, *Principles of Abrasive Water Jet Machining*. Springer London (1998).
- [26] J.W. Hoyt, J.J. Taylor, Turbulence structure in a water jet discharging in air. *Physics of Fluids* **20** (10), S253-S257 (2008). DOI: <https://doi.org/10.1063/1.861738>
- [27] Y. Hu, A.Y. Cao, X.F. Qin, C.C. Xue, W.H. Guo, Y.Q. Liu, Y.J. Peng, Study on Optimization of water jet slit pressure relief parameters in deep rock burst coal seam. *Journal of Geotechnical Engineering* 1-8 (2022-08-18). <http://kns.cnki.net/kcms/detail/32.1124.TU.20220817.1359.004.html>
- [28] T. Orlando, C. Valentina, V. Marco, Equation-Based Modelling: True Large Strain, Large Displacement and Anand's Plasticity Model with The ComSol Deformed Mesh Module// European COMSOL Conference 2009. COMSOL Inc. (2009). *International Symposium on Plasticity and Impact Mechanics*
- [29] P. Franciosa, S. Gerbino, Handling Tesselated Free Shape Objects with a Morphing Mesh Procedure in Comsol Multiphysics// Comsol 2009. *International Symposium on Plasticity and Impact Mechanics*.
- [30] R.G. Hou, Wang, Z. Lv, Y.B. Tian, Numerical simulation of magnetic field assisted abrasive water jet flow field distribution based on COMSOL. *Aerospace Manufacturing Technology* **62** (18), 43-49 (2019). DOI: <https://doi.org/10.16080/j.issn1671-833x.2019.18.043>
- [31] M. Chen, Z.X. Chen, R.Z. Huang, Three dimensional bending hydraulic fracture mechanical model and calculation method. *Journal of Petroleum University (Natural Science Edition)* (S1), 43-47 (1995). DOI: <https://doi.org/10.1016/j.jrmmms.2018.01.010>